Carcinogenesis vol.29 no.4 pp.713–721, 2008
doi:10.1093/carcin/bgn032
Advance Access publication February 6, 2008

Reactive oxygen species stabilize hypoxia-inducible factor-1 alpha protein and stimulate transcriptional activity via AMP-activated protein kinase in DU145 human prostate cancer cells

Seung-Nam Jung, Woo Kyeom Yang, Joungmok Kim, Hak Su Kim, Eun Ju Kim, Hee Yun, Hyunsung Park[1], Sung Soo Kim, Wonchae Choe, Insug Kang* and Joohun Ha

Department of Biochemistry and Molecular Biology, Kyung Hee University School of Medicine, Seoul 130-701, Korea and [1]Department of Life Science, University of Seoul, Seoul 130-743, Korea

*To whom correspondence should be addressed. Tel: +82 2 961 0922;
Fax: +82 2 965 6349;
Email: iskang@khu.ac.kr
Correspondence may also be addressed to Joohun Ha. Tel: +82 2 961 0921;
Fax: +82 2 959 8168;
Email: hajh@khu.ac.kr

Hypoxia-inducible factor (HIF-1) plays a central role in the cellular adaptive response to hypoxic conditions, which are closely related to pathophysiological conditions, such as cancer. Although reactive oxygen species (ROS) have been implicated in the regulation of hypoxic and non-hypoxic induction of HIF-1 under various conditions, the role of ROS is quite controversial, and the mechanism underlying the HIF-1 regulation by ROS is not completely understood yet. Here, we investigated the biochemical mechanism for the ROS-induced HIF-1 by revealing a novel role of adenosine monophosphate-activated protein kinase (AMPK) and the upstream signal components. AMPK plays an essential role as energy-sensor under adenosine triphosphate-deprived conditions. Here we report that ROS induced by a direct application of H_2O_2 and menadione to DU145 human prostate carcinoma resulted in accumulation of HIF-1α protein by attenuation of its degradation and activation of its transcriptional activity in an AMPK-dependent manner. By way of contrast, AMPK was required only for the transcriptional activity of HIF-1 under hypoxic condition, revealing a differential role of AMPK in these two stimuli. Furthermore, our data show that inhibition of AMPK enhances HIF-1α ubiquitination under ROS condition. Finally, we show that the regulation of HIF-1 by AMPK in response to ROS is under the control of c-Jun N-terminal kinase and Janus kinase 2 pathways. Collectively, our findings identify AMPK as a key determinant of HIF-1 functions in response to ROS and its possible role in the sophisticated HIF-1 regulatory mechanisms.

Introduction

Hypoxia initiates a series of adaptive responses via the coordinated upregulation of genes involved in angiogenesis, erythropoiesis and glycolysis, and many of these responses are mediated by hypoxia-inducible factor-1 (HIF-1) (1). HIF-1 is a heterodimeric transcription factor composed of HIF-1α and HIF-1β (2). Under normoxic conditions, HIF-1 is targeted for degradation by a set of enzymes known as a prolyl hydroxylase (PHD) that utilize oxygen as a substrate and iron, Fe^{2+}, as a cofactor to hydroxylate the proline residues (Pro^{402} and Pro^{564}) on HIF-1α (3–5). Hydroxylation of HIF-1α promotes to interact with the von Hippel-Lindau protein (pVHL), which has E3 ubiquitin ligase activity and leads to degradation of HIF-1α (6). However, as oxygen concentration declines, HIF-1α is rapidly stabilized as a result of blockade of prolyl hydroxylation.

Because oxygen is a main component of reactive oxygen species (ROS), such as superoxide and peroxide, ROS have been thus implicated as an oxygen sensor and thereby linked to the regulation of HIF-1 under the limited oxygen supply. Moreover, accumulating evidences have demonstrated that HIF-1 also responds to non-hypoxic stimuli such as hormones, growth factors, vasoactive peptides and cytokines (7), and ROS were also suggested to play a critical role in HIF-1 expression under non-hypoxic conditions (8,9). However, there are acute controversies regarding whether ROS levels increase or decrease during hypoxic conditions (10–12). Moreover, ROS appear to have dual effects on HIF-1: a number of reports highlighted the role of ROS for HIF-1α inductions (13–15), but ROS have also been demonstrated to be able to destabilize HIF-1α under hypoxic and non-hypoxic conditions (16–18). Consequently, the regulatory mechanisms by which HIF-1 is regulated by ROS under hypoxic or non-hypoxic conditions seem to be highly complex and are not completely known yet.

Similar to the oxygen and/or ROS level, the cellular energy status is also one of critical regulatory cues to maintain cellular function and integrity (19). Adenosine monophosphate-activated protein kinase (AMPK), a heterotrimeric enzyme consisting of a catalytic subunit (α) and two regulatory subunits (β and γ), plays a critical role as an energy sensor in various stresses causing the depletion of intracellular adenosine triphosphate (ATP) such as hypoxia and ROS (20,21). In a previous study, we reported that AMPK activity is critical for the regulation of transcriptional activity of HIF-1 under hypoxic condition in various cancer cells (22). In addition, we have shown that AMPK contributes to increases in the stability of vascular endothelial growth factor (VEGF) mRNA in cancer cells under glucose-deprivation conditions (23). The results collectively suggest that the AMPK-mediated energy-sensing signal is probably to be integrated to the adaptive responses of cancer cells in responses to various stress conditions.

In the present study, we examined the biochemical mechanisms for the ROS-induced HIF-1 expression in DU145 human prostate carcinoma by primarily focusing on the role of AMPK and by revealing novel upstream signal components.

Abbreviations: ACC, Acetyl-CoA Carboxylase; Ad-AMPK-DN, AMPK dominant negative form; AMPK, adenosine monophosphate-activated protein kinase; ATP, adenosine triphosphate; ERK, extracellular signal-regulated kinase; GSK-3, glycogen synthase kinase-3; HIF-1, hypoxia-inducible factor-1; JAK2, Janus kinase 2; JNK, c-Jun N-terminal kinase; NAC, N-acetyl-cysteine; PHD, prolyl hydroxylase; pVHL, von Hippel-Lindau protein; ROS, reactive oxygen species; STAT, signal transducers and activators of transcription; VEGF, vascular endothelial growth factor.

Materials and methods

Materials

The RPMI 1640 and fetal bovine serum were purchased from Life Technologies (Grand Island, NY). Cycloheximide, MG132, catalase, N-acetyl-cysteine (NAC), potassium dichromate, ethyl 3,4-dihyrdoxybenzoate and desferoxamine were obtained from Sigma-Aldrich (St. Louis, MO). PD98059, SP600125, SB203580, LY294002 and AG490 were from TOCRIS (Bristol, UK). Compound C was from Calbiochem (San Diego, CA). The antibodies specific to phosphoactive form P-Acetyl-CoA carboxylase (ACC), P-AMPK, P-ERK, P-JNK, P-p38, P-AKT, P-c-Jun, P-STAT3 and P-GSK-3α/β were obtained from Cell Signaling (Beverly, MA). The antibodies against ACC, HIF-1β, c-myc and α-actinin were purchased from Santa Cruz (Santa Cruz, CA). Antibody for HIF-1α was obtained from BD Bioscience (San Jose, CA) and Santa Cruz. AMPKα antibody was purchased from Upstate Biotechnology (Lake Placid, NY). Plasmid pEpoE-luc, pcDNA3-JNK1 and pRK-JAK2 were generously provided by Dr Franklin Bunn (Harvard Medical School, MA), Dr Roger J. Davis (University of Massachusetts, MA) and Dr David E. Levy (New York University, NY). Plasmid pCMV-HA-ubiquitin and pCR3-HA-pVHL were generously provided by Dr Hong-Duk Youn (Seoul National University, Korea).

Cell culture

DU145 (human prostate carcinoma), HeLa (cervix carcinoma), A549 (lung carcinoma), HCT116 (colon carcinoma) and HepG2 (hepatocellular liver carcinoma) were maintained in RPMI 1640 supplemented with 10% fetal bovine

serum and antibiotics at 37°C with 95% air and 5% CO_2. For hypoxic condition, cells were transferred to a Bactron Anaerobic/Environmental Chamber (Sheldon Manufacturing, Inc. Cornelius, OR), which was flushed with 1% O_2, 5% CO_2 and 95% N_2 at 37°C.

Immunoblotting and immunoprecipitation

After the indicated treatments, cells were washed with ice-cold phosphate-buffered saline and lysed in RadioImmunoPrecipitation Assay buffer. After centrifugation at 14 000 r.p.m. for 15 min, the supernatant was collected. For immunoprecipitation, 500 μg of protein extracts were incubated with an antibody coupled to protein G-agarose at 4°C for 2 h. The immunocomplex was recovered by a centrifugation and washed with phosphate-buffered saline containing 0.5 M NaCl and 0.5% Noniodet-P40. The samples were resolved on sodium dodecyl sulfate–polyacrylamide gel electrophoresis, transferred onto nitrocellulose membrane and then were detected by enhanced chemiluminescence substrate reagent in autoradiographs.

Adenovirus-mediated gene transfer

c-myc-tagged AMPK wild-type α subunit and a dominant negative form were generated, prepared and purified as described previously (22). Infections with adenovirus expressing AMPK wild-type (Ad-AMPK-WT) and AMPK dominant negative form (Ad-AMPK-DN) were conducted in phosphate-buffered saline for 30 min at 37°C, after which fresh medium was added.

Transfection and HIF-1 reporter assays

Cells were plated onto 24-well culture plates (1×10^4 cells/well) or 6-well plates (5×10^5 cells/well), and the following day transfections were conducted as described previously (24). Two micrograms of each plasmid were transfected into cells and 24–48 h later indicated treatments were performed. The resulting luciferase activity was measured by luminometer (TD-20/20 luminometer).

RNA isolation and reverse transcription–polymerase chain reaction

Total RNA was extracted with Trizol reagent, and reverse transcription–polymerase chain reaction was performed as described previously (22). The corresponding gene fragments were amplified by polymerase chain reaction using specific primers for HIF-1α (sense, 5′-CTTGCTCATCAGTTGCCACTT; antisense, 5′-GCCATTTCTGTGTGTAAGCAT), VEGF (sense, 5′-AGGAGGGCAGAATCATCACG; antisense, 5′-CAAGGCCCACAGGGATTTTCT) and β-actin (sense, 5′-GTGGGGCGCCCAGGCACCA; antisense, 5′-CTCCTTAATGTCACGCACCATTTC). The amplified products were visualized on 1% agarose gels.

[^{35}S] Metabolic labeling

Total of 3×10^5 cells were plated in a 60 mm dish, and 24 h later, culture medium was replaced with [^{35}S]methionine/cysteine-free media containing 5% serum for 30 min. Thereafter, [^{35}S]methionine/cysteine was added to a final concentration of 0.2 mCi/ml, and the cells were pulse labeled for 1 h under H_2O_2, hypoxia, insulin and then harvested. An equal amount of protein extract was immunoprecipitated with anti-HIF-1α antibody. The released proteins were separated on 8% sodium dodecyl sulfate–polyacrylamide gel electrophoresis gel and autoradiographed.

HIF-1α polyubiquitination and HIF-1α–pVHL interaction assay

HEK293 cells were cotransfected with 0.5 μg of pCMV-HA-ubiquitin plasmid and 0.5 μg of pCR3-HA-pVHL plasmid. After 1 day post-transfection, cells were treated with H_2O_2 in the presence or absence of MG132, for 30 min. Cells were harvested and lysed, and 500 μg of cell extracts were incubated with 2 μg of anti-HIF-1α antibody coupled with protein G-agarose for 2 h at 4°C. After washing the immunocomplex, ubiquitination and HIF-1α–pVHL interaction were determined by immunoblotting.

Statistical analysis

Results are expressed as the means ± standard error. We used Student's *t*-test. Differences were considered significant at a P value of <0.05.

Results

ROS induce HIF-1α expression and AMPK activation in DU145 human prostate carcinoma

To investigate a role of ROS in the regulation of HIF-1α expression, DU145 human prostate carcinomas were exposed to the indicated concentration of H_2O_2 or menadione, a well-known generator of superoxide anion (25), for 1 h in culture media containing 10% fetal bovine serum, and then we examined the HIF-1 protein level (Figure 1). HIF-1α expression was induced in a concentration-dependent manner, showing a maximal induction at the concentration of 0.5 mM H_2O_2 (Figure 1A) or 100 μM menadione (Figure 1B). As exposure of DU145 cells to these concentrations of H_2O_2 or menadione in 10% serum-containing media for 24 h did not result in any significant induction of cell death (data not shown), we used 0.5 mM H_2O_2 or 100 μM menadione for inducing HIF-1α expression throughout the present study. Time course study indicated that HIF-1α expression was rapidly induced within 1 h in response to both H_2O_2 and menadione, and the protein induction was sustained for 4–8 h. The time course pattern was quite similar to that seen in DU145 cells exposed to hypoxia (1% O_2) (Figure 1C). Under these conditions, HIF-1β protein level was constant. Both H_2O_2 and menadione also activated AMPK in a dose-dependent manner, as evidenced by the phosphorylation level of Thr^{172} in the active site of AMPKα catalytic subunit, which is known to be essential to enzyme activity. Also, phosphorylation of Ser^{79} of ACC, which is well-characterized phosphorylation site by AMPK, was concomitantly increased. Since AMPK is known to be activated sensitively under ATP-depletion conditions (19) and we thus measured the levels of intracellular ATP in cells under ROS and hypoxia conditions. Time course study showed that the decreased ATP levels (Figure 1D) appeared to be correlated with AMPK activation (Figure 1A–C). Collectively, these results indicate that both ROS and hypoxia rapidly induced HIF-1α expression as well as AMPK activation in DU145 cells.

Inhibition of AMPK activity abrogates ROS-induced HIF-1α protein, but not hypoxia-induced one

Similar temporal profiles of AMPK activation and HIF-1α expression between ROS and hypoxia conditions prompted us to compare the role of AMPK in HIF-1α expression. To this end, we have taken a pharmacological and molecular approach to inhibit the AMPK activity under ROS and hypoxia condition, and then examined its subsequent effect on HIF-1α protein levels, its transcriptional activity and the target gene expressions in DU145 cells (Figure 2). Pretreatment with compound C (20 μM) for 30 min, a potent and selective inhibitor for AMPK (26) (Figure 2A), or adenovirus-mediated expression of c-myc-tagged Ad-AMPK-DN (Figure 2B), effectively blocked H_2O_2-, menadione- and hypoxia-induced AMPK activation, as evidenced by the phosphorylation level of ACC-Ser^{79}. However, inhibition of AMPK activity specifically abrogated only H_2O_2- and menadione-induced HIF-1α expression, but not hypoxia-induced HIF-1α expression (Figure 2A and B). The differential effects of AMPK on ROS- and hypoxia-induced HIF-1α accumulation were also observed in various cancer cell lines, including HeLa cervix carcinoma, A549 lung carcinoma, HCT116 colon carcinoma and HepG2 hepatocellular liver carcinoma (Figure 2C). Although both H_2O_2 and hypoxia rapidly activated AMPK (data not shown) and increased HIF-1α protein levels in these cell lines, only H_2O_2-induced HIF-1α expression was suppressed by inhibition of AMPK activation. Therefore, AMPK-dependent HIF-1α expression in response to ROS is probably to be quite a widespread phenomena rather than certain cell type specific.

To gain further insight into the differential effect of AMPK inhibition in the context of ROS- and hypoxia-induced HIF-1α protein levels, we then investigated the effect of AMPK inhibition on HIF-1 transcriptional activity. DU145 cells were transiently transfected with a plasmid (pEpoE-luc) containing a luciferase reporter driven by the human erythropoietin HIF-1 binding site (5′-TACGTGCT-3') and SV40 promoter. After 24 h post-transfection, cells were exposed to H_2O_2, menadione or hypoxia for an additional 6 h in the presence or absence of AMPK inhibitor. H_2O_2, menadione and hypoxia significantly induced the HIF-1-dependent luciferase activities by up to ~4- to 5-fold, and the induced HIF-1 activity was diminished substantially by an AMPK inhibitor compound C (Figure 2D). These results were confirmed when endogenous AMPK activity was blocked by infection with Ad-AMPK-DN. In accordance with HIF-1 transcriptional activity, the VEGF mRNA level, which is a major target gene of HIF-1 transcriptional factor, was distinctively increased in response to

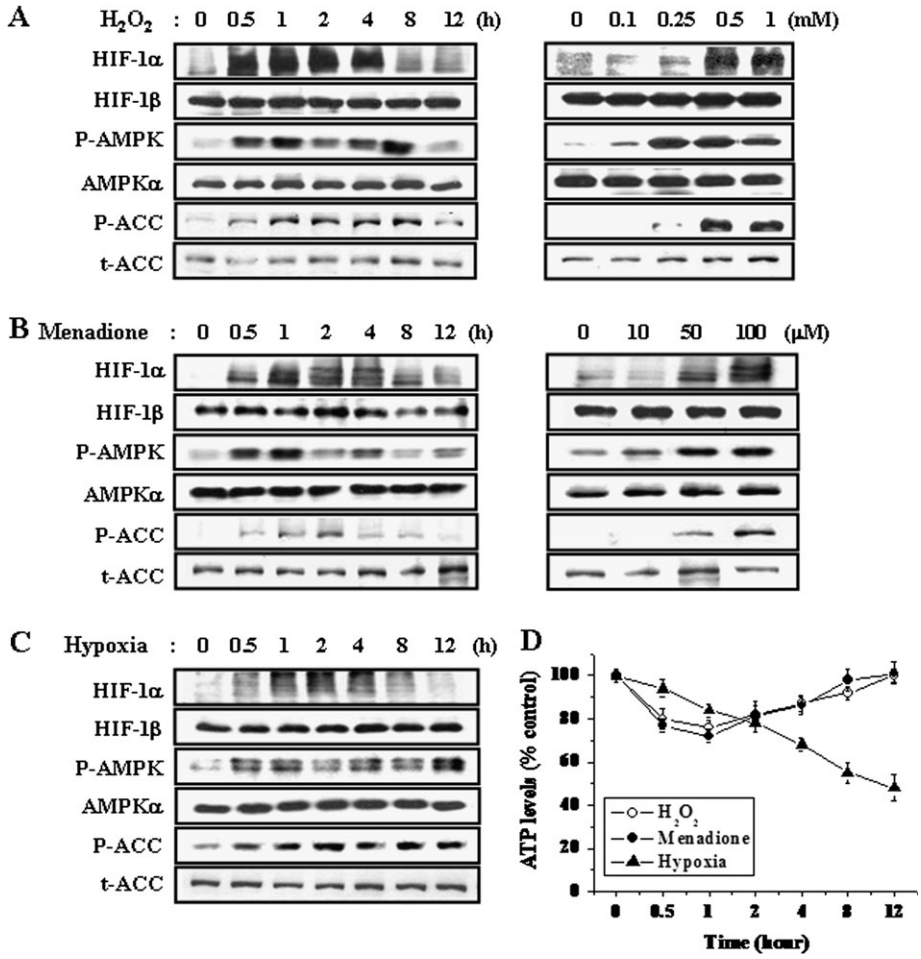

Fig. 1. ROS stimulate AMPK activation and HIF-1α induction. DU145 cells were treated with 0.5 mM H_2O_2 (**A**) or 100 μM menadione (**B**) or exposed to 1% hypoxia (**C**) for the indicated time period. Also, cells were incubated with the indicated concentration of H_2O_2 (0–1 mM) or menadione (0–100 μM) for 1 h. Under these conditions, the total cell extracts were subjected to western blot assays using anti-phosphospecific AMPKα-Thr^{172} (P-AMPK), anti-AMPKα (AMPK-α), anti-phosphospecific ACC-Ser^{79} (P-ACC), anti-ACC (t-ACC), anti-HIF-1α (HIF-1α) and anti-HIF-1β (HIF-1β) antibody. (**D**) Cells were treated with 0.5 mM H_2O_2, 100 μM menadione or 1% hypoxia for the indicated times, and the cellular ATP concentrations were measured by the luciferase/luciferin method using an ATP Determination Kit (Sigma-Aldrich, St. Louis, MC).

H_2O_2, menadione and hypoxia for 6 h, and the inhibition of AMPK effected significant reductions in the levels of VEGF mRNA (Figure 2D). Thus far, our data have shown that AMPK activity is required for ROS-induced HIF-1α expression, but not for hypoxia-induced HIF-1α expression. Nevertheless, AMPK activity appears to be required for the hypoxia-induced HIF-1 transcriptional activity.

ROS induce the accumulation of HIF-1α protein by attenuation of its degradation through an AMPK-dependent pathway

Findings of recent studies suggest that a number of growth factors including insulin also induce HIF-1α expression under normoxic conditions (27). In this case, the increased rate of HIF-1α protein synthesis has been implicated for the mechanism of HIF-1α induction. Therefore, to understand the molecular mechanism by which ROS induce HIF-1α expression, we first performed the metabolic labeling experiments to investigate whether H_2O_2 can induce HIF-1α protein synthesis and compared the results with insulin-treated conditions. DU145 cells were serum-starved for 5 h, and then exposed to H_2O_2 (0.5 mM) or insulin (100 ng/ml) for 2 h. Then, cells were labeled for additional 1 h in methionine-free media containing [^{35}S]methionine/cysteine (0.3 mCi/ml), followed by immunoprecipitation of HIF-1α (Figure 3A). As expected, ^{35}S-labeled HIF-1α was distinctively observed in insulin-treated cells in contrast to the control cells, whereas ^{35}S-labeled HIF-1α was not detected in cells exposed to H_2O_2. Under these conditions, HIF-1α mRNA levels were not altered. These results suggest that HIF-1α protein accumulation induced by ROS occurs at post-translational step.

On the basis of the results obtained so far, we reasoned that ROS could induce HIF-1α protein stabilization, and we thus investigated the kinetics of HIF-1α decay in the presence of cycloheximide, a protein synthesis inhibitor. After exposure of DU145 cells to H_2O_2, hypoxia or insulin for 1 h, cycloheximide was added to the cells with final concentration (50 μM), and cells were further incubated for additional 90 min (Figure 3B). HIF-1α protein in insulin-treated cell rapidly degraded when protein synthesis was blocked by cycloheximide, and practically no protein was detected in 90 min exposure to cycloheximide, supporting the notion that growth factor such as insulin can induce HIF-1α expression under normoxic condition via increasing the rate of the protein synthesis. In contrast, the HIF-1α in hypoxia-induced cells appeared to be relatively stable, and ~70 to 80% of the protein was still detectable after 90 min exposure to cycloheximide, thus indicating that hypoxia stabilizes HIF-1α by blocking its degradation. Interestingly, HIF-1α induced by H_2O_2 seemed to be more stable than hypoxia-induced one: the HIF-1α protein level in H_2O_2-treated cells practically did not alter >90 min in the presence of cycloheximide. These results suggest that the stabilization of HIF-1α is a main mechanism for the protein accumulation in response to H_2O_2.

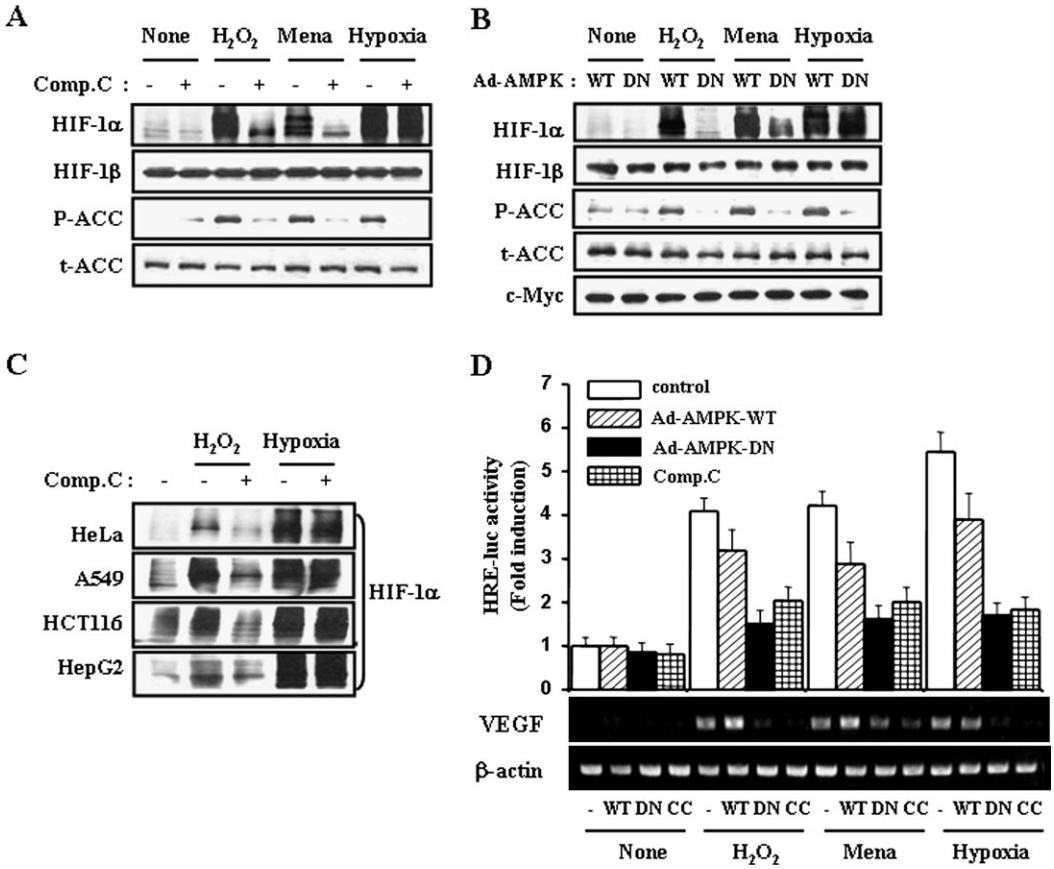

Fig. 2. Inhibition of AMPK diminishes the ROS-induced HIF-1α induction, but not hypoxia-induced HIF-1α induction. DU145 cells were either pretreated with 20 μM compound C (Comp.C) for 20 min (**A**) or infected with adenovirus expressing AMPKα wild-type (Ad-AMPK-WT) or dominant negative (Ad-AMPK-DN) (**B**). These cells were then exposed to H_2O_2 (0.5 mM), menadione (100 μM, Mena) and hypoxia (1% O_2) for 1 h, and then phosphorylation level of ACC-Ser^{79} (P-ACC), total amount of ACC (t-ACC), HIF-1α and HIF-1β were analyzed by western blot. (**C**) Hela, A549, HCT116 and HepG2 cells were treated with H_2O_2 (0.5 mM) and hypoxia (1% O_2) for 1 h in the absence or presence of 20 μM compound C (Comp.C). The protein level of HIF-1α was determined by western blot. (**D**) After 24 h post-transfection with a plasmid (pEpoE-luc) harboring a luciferase reporter driven by the human erythropoietin HIF-1 binding site, DU145 cells were treated with compound C or infected with adenovirus in an identical manner as in (A) and (B). After exposure to H_2O_2 (0.5 mM), menadione (100 μM, Mena) and hypoxia (1% O_2) for 6 h, luciferase activity was measured. Results are the mean ± standard error of at least four independent experiments (upper panel). Under identical conditions, the mRNA level of VEGF and β-actin were determined by reverse transcription–polymerase chain reaction, and the amplified products were analyzed on 1% agarose gel (lower panel).

Next, in order to clearly demonstrate the role of AMPK in the regulation of H_2O_2-induced HIF-1α, we determined the turnover rate of HIF-1α protein after blocking protein synthesis in DU145 cells expressing a wild type or a dominant negative form of AMPK. As shown in Figure 3C, HIF-1α protein level, which was induced by H_2O_2, was significantly reduced by Ad-AMPK-DN. Moreover, in contrast to the cells expressing AMPK wild type, cycloheximide addition after H_2O_2 treatment resulted in a rapid reduction of half-life of HIF-1α protein (<15 min) in cells expressing Ad-AMPK-DN. These results collectively demonstrate that AMPK plays a critical role in HIF-1α protein stabilization induced by H_2O_2.

ROS stimulate HIF-1 trans-activation ability through AMPK activation

Since there are some controversial reports describing the role of ROS in hypoxia-induced HIF-1α induction, we examined the intracellular ROS levels on the exposure to hypoxia using 2′,7′-dichlorofluorescein diacetate staining and found that ROS levels were not increased at 1 h incubation under hypoxia (data not shown). Consistent with this result, pretreatment with antioxidants including catalase and N-acetyl cysteine (NAC) does not affect HIF-1α induction in the cells exposed to hypoxia for 1 h, whereas H_2O_2-induced HIF-1α accumulation was dramatically reduced by catalase or NAC (Figure 4A). In addition, to demonstrate that AMPK activation by ROS produced under pathophysiological condition mediates HIF-1α protein accumulation, we showed that a carcinogenic metal chromium, Cr (VI), which has been shown to induce HIF-1 through ROS generation in DU145 cells (28), induced AMPK activation and HIF-1α proteins and that compound C as well as catalase and NAC inhibited HIF-1α protein levels (Figure 4B).

We next investigated whether ROS stimulate the *trans*-activation ability of HIF-1. To this end, we first compared the effect of H_2O_2 on HIF-1α protein level with that of MG132, a well-known inhibitor of 26S proteasome inhibitor. Treatment with both MG132 (100 μM) and H_2O_2 for 1 h resulted in distinctive induction of HIF-1α expression in DU145 cells, and a higher level of HIF-1α appeared to be accumulated by MG132 treatment (Figure 4C, upper panel). Nevertheless, the luciferase activity derived from transfection of pEpoE-luc was significantly higher in cells treated with H_2O_2 than MG132 (Figure 4C, lower panel), thereby suggesting that H_2O_2 may increase the transcriptional activity of HIF-1. In order to directly address this possibility, we used a GAL4-driven reporter system, which can only measure the *trans*-activation ability of HIF-1α (29). Because only the GAL4 fusion protein is able to bind GAL4 binding site of pGAL4-tk-luc after cotransfection with pGAL4-tk-luc and pGAL4/HIF-1α, the luciferase is expressed only when HIF-1α has a *trans*-activation ability. DU145 cells were cotransfected with pGAL4/HIF-1α and pGAL4-tk-luc, and then exposed to H_2O_2, menadione, hypoxia or MG132 for 6 h (Figure 4D). In contrast to treatment with

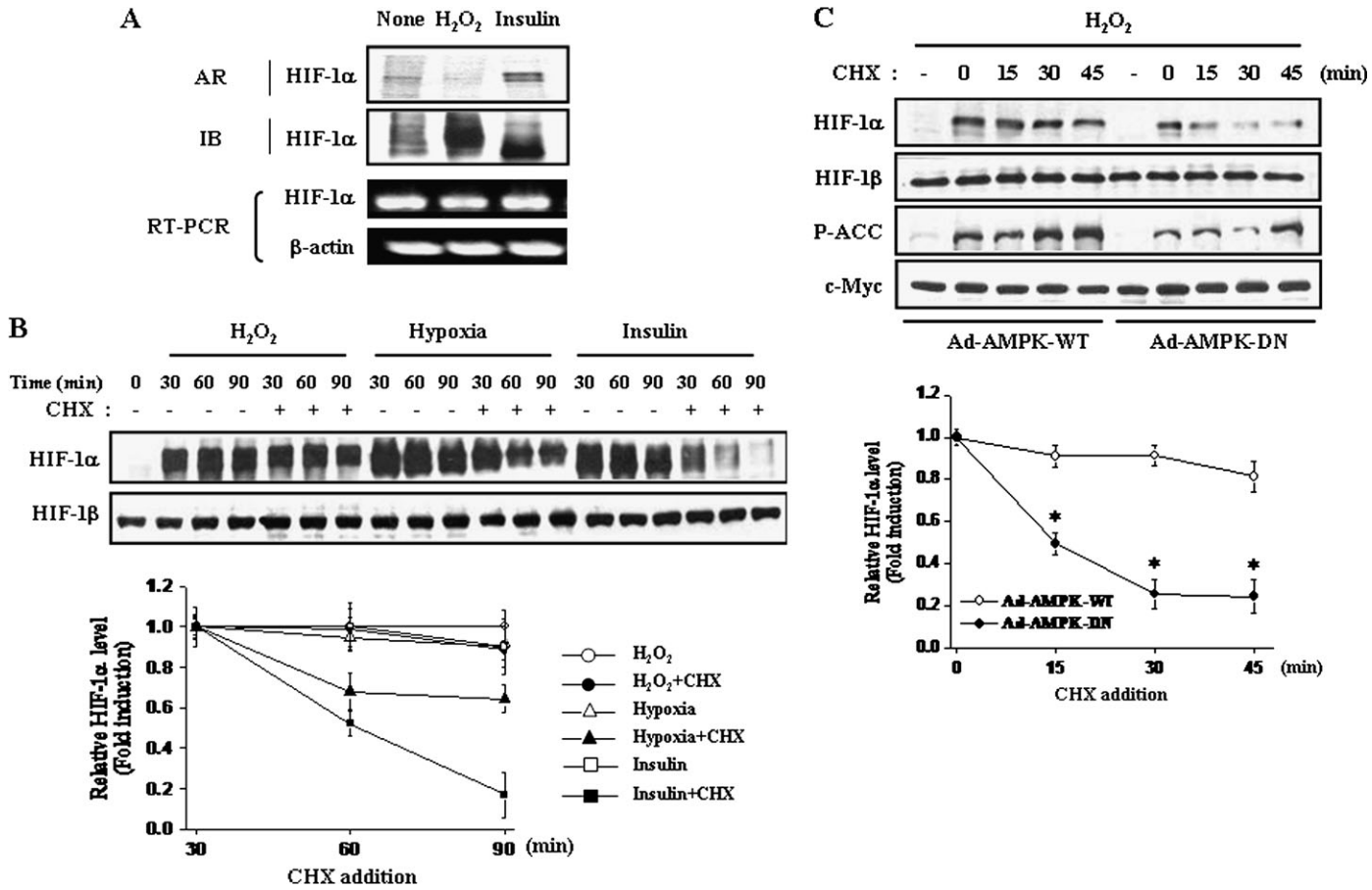

Fig. 3. ROS stabilize HIF-1α protein in AMPK-dependent manner. (**A**) DU145 cells were labeled with ^{35}S-methionine/cystein during 1 h exposure to either H_2O_2 (0.5 mM) or insulin (0.5 μM) as described in Materials and Methods section. Whole-cell extracts (1 mg) were immunoprecipitated using an anti-HIF-1α antibody. The samples were then analyzed by sodium dodecyl sulfate–polyacrylamide gel electrophoresis (8%) followed by autoradiography (AR) or immunoblotted using an anti-HIF-1α antibody (IB). The mRNA levels of HIF-1α and β-actin were compared by reverse transcription–polymerase chain reaction. (**B**) DU145 cells were exposed to 0.5 mM H_2O_2, 1% hypoxia or 0.5 μM insulin for 1 h, and cycloheximide (CHX) was then added to final concentration 50 μM and further incubated for 90 min. Then, the protein level of HIF-1α and HIF-1β was determined by immunoblot analysis. The protein level of HIF-1α was compared with that of 30 min point of cycloheximide addition and was expressed as a fold induction in a lower graph. Results are the mean ± standard error (SE) of four independent experiments. (**C**) DU145 cells were infected with Ad-AMPK-WT or Ad-AMPK-DN. The cells were challenged with 0.5 mM H_2O_2 for 1 h and then cells were further incubated for the indicated time period in the presence of 50 μM CHX. Protein turnover of HIF-1α and HIF-1β under the inhibition of protein synthesis by CHX was monitored by immunobloting. Also, H_2O_2-induced AMPK activation was determined by the phosphorylation level of its cellular substrate ACC (P-ACC). Expression of AMPKs in adenoviral-infected cells was confirmed by immunoblotting against their N-terminal c-myc tag using anti-c-myc antibody (c-Myc). The protein level of HIF-1α was compared with that of 0 min point of cycloheximide addition and was expressed as a fold induction in a lower graph. Results are the mean ± SE of four independent experiments ($^*P < 0.01$; compared with Ad-AMPK-WT).

MG132, which failed to increase luciferase expression, the treatment with H_2O_2, menadione and hypoxia resulted in stimulation of the reporter expression ∼2-fold, and this activation was almost completely blocked by AMPK inhibitor compound C. Consequently, these results suggest that H_2O_2 also stimulates HIF-1 *trans*-activation ability via AMPK activation.

Inhibition of AMPK enhances HIF-1α ubiquitination by increasing its interaction with pVHL in response to H_2O_2

To understand the mechanism by which AMPK stabilizes HIF-1α protein, we first examined the effect of AMPK activity on the HIF-1α ubiquitination and its interaction with pVHL under H_2O_2 and hypoxia. To do this, HEK293 cells were transfected with plasmids for HA-tagged ubiquitin and HA-tagged pVHL for 24 h and were then treated with H_2O_2 or hypoxia in the presence of MG132. Cell lysates were then immunoprecipitated with anti-HIF-1α antibody and were immunobloted with either anti-HA antibody or anti-HIF-1α antibody. As shown in Figure 5A, both H_2O_2 and hypoxia decreased HIF-1α ubiquitination, as compared with untreated control cells. AMPK inhibition by compound C markedly increased HIF-1α ubiquitination and HIF-1α–pVHL interaction in response to H_2O_2, whereas it did not significantly affect HIF-1α ubiquitination and HIF-1α–pVHL interaction under hypoxia (Figure 5A). This result suggests that ROS-activated AMPK inhibits HIF-1α ubiquitination by preventing its interaction with pVHL and consequently induces HIF-1α protein accumulation.

We next examined whether AMPK exerts its effect on HIF-1α ubiquitination and protein stability through modulating PHD enzyme. Among three PHDs (PHD 1–3) identified in mammals, PHD2 is known as the critical oxygen sensor and its expression has been reported to be altered under different hypoxic or normoxic condition in DU145 cells (30). However, we found that PHD2 expression did not change at 1 h incubation of cells with both H_2O_2 and hypoxia (Figure 5B) and longer treatment of cells with H_2O_2 also did not affect PHD2 protein levels (Figure 5C). Moreover, previous other studies show that enhanced ROS levels inhibit PHD activity by promoting oxidation of a cofactor of PHD Fe^{2+} to Fe^{3+} (31). To this end, DU145 cells were pretreated with pharmacological inhibitors of PHDs, ethyl 3,4-dihyrdoxybenzoate and desferoxamine with or without compound C,

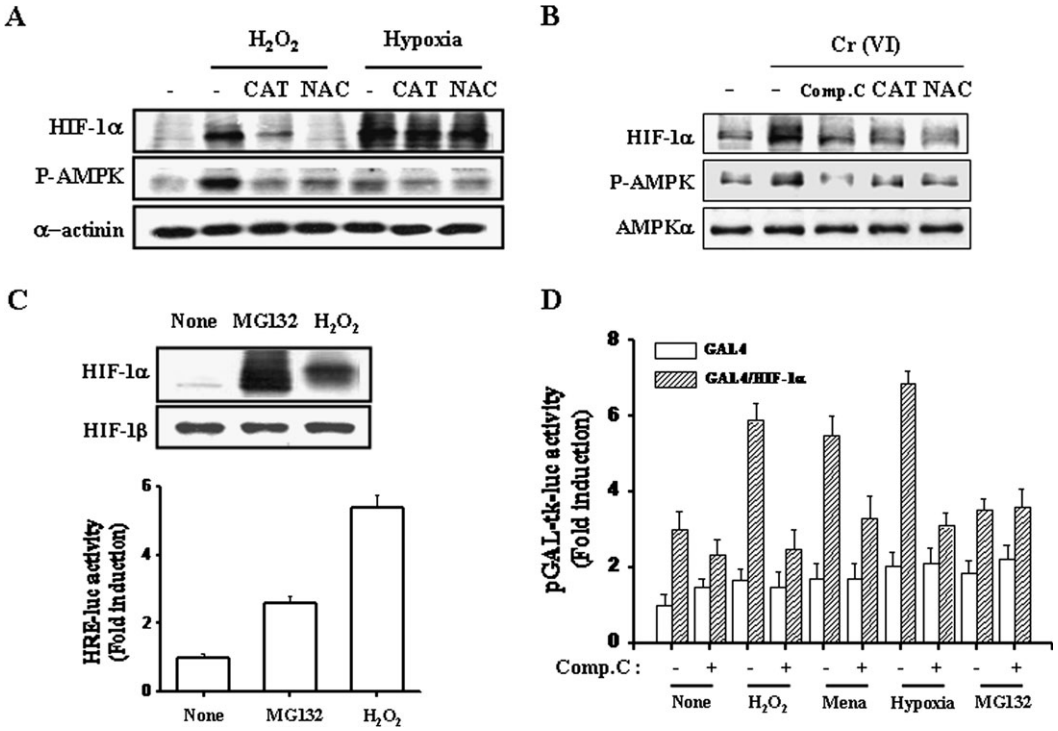

Fig. 4. Roles of ROS and AMPK in HIF-1α protein and transcriptional activity. (**A**) DU145 cells were exposed with 0.5 mM H_2O_2 and 1% hypoxia for 1 h in the presence or absence of catalase (3000 units/ml) or NAC (10 mM) for 1 h. (**B**) DU145 cells were treated with 5 μM potassium dichromate [Cr (VI)] for 3 h in the presence or absence of 20 μM compound C (Comp.C), catalase and NAC for 1 h. The protein levels of HIF-1α and α-actinin and the phosphorylation level of AMPK were determined by immunoblotting. (**C**) DU145 cells were exposed 0.5 mM H_2O_2 or 10 μM MG132 for 1 h, and then total cell extracts were prepared. Protein levels of HIF-1α and HIF-1β were determined by immunoblot analysis (upper panel). DU145 cells were transiently transfected with pEpoE-luc plasmid harboring a luciferase reporter gene under HIF-1 response element. After 24 h post-transfection, cells were exposed to 0.5 mM H_2O_2 or 10 μM MG132 for an additional 6 h. Protein extracts were prepared and subjected to the luciferase activity assay (lower panel). (**D**) DU145 cells were cotransfected with a plasmid pGAL4 or pGAL4/HIF-1α and a reporter plasmid (pGAL-tk-luc) with a 1:1 molar ratio. The following day, the cells were treated with 0.5 mM H_2O_2, 100 μM menadione (Mena), 1% hypoxia or 10 μM MG132 in the presence or absence of 20 μM compound C (Comp.C). After 6 h incubation, cells were harvested and subjected to measure the luciferase activities. The data represent mean ± standard error for three independent experiments.

and then HIF-1α protein levels were examined under H_2O_2 and hypoxia condition. The results showed that in the presence of ethyl 3,4-dihyrdoxybenzoate or desferoxamine, HIF-1α protein levels were enhanced in basal as well as both H_2O_2 and hypoxia condition compared with untreated control cells (Figure 5D). Importantly, in the presence of PHD inhibitors, AMPK inhibition by compound C still significantly reduced HIF-1α protein level under H_2O_2, which was not observed in cells under hypoxia (Figure 5D). Collectively, these results suggest that AMPK-dependent pathway is stronger than inhibition of PHD for the HIF-1α protein stabilization under both basal and ROS condition in DU145 cells.

c-Jun N-terminal kinase and Janus kinase 2 act as upstream components for the AMPK signaling pathway leading to HIF-1α induction in response to H_2O_2

We next attempted to elucidate the signaling pathway underlying H_2O_2-induced HIF-1α by examining a cross talk between AMPK and extracellular signal-regulated kinase (ERK), p38, c-Jun N-terminal kinase (JNK), phosphatidylinositol 3-kinase/AKT and Janus kinase–signal transducers and activators of transcription (JAK–STAT) pathways. These kinases were previously implicated in stabilization or activation of HIF-1 under various conditions (32–37). To this end, the activation kinetics of these kinases in response to H_2O_2 was initially determined by examining the level of the phosphoactivated form of each kinase or the phosphorylation level of the substrate of the kinase. Immunoblot analyses revealed that phosphoactivated form of ERK, p38, JNK, AKT and STAT3 were detected in response to H_2O_2 in DU145 cells (Figure 6A). Under these conditions, the total form of each protein was not altered (data not shown). In order to test the involvement of each kinase on HIF-1α induction, DU145 cells were pretreated for 30 min with a specific kinase inhibitor for each kinase (PD98059 for ERK, SP600125 for JNK, SB202190 for p38, LY294002 for phosphatidylinositol 3-kinase/AKT and AG490 for JAK2), and then exposed to H_2O_2 for 1 h. Among them, JNK inhibitor (SP600125) and JAK2 inhibitor (AG490) led to a significant reduction in H_2O_2-induced phosphorylation levels of AMPK and ACC and the protein level of HIF-1α (Figure 6B). In contrast, inhibition of AMPK with compound C did not affect the activations of all of tested kinases as well as glycogen synthase kinase-3 (GSK-3) a downstream of AKT (Figure 6C), suggesting that JNK and JAK2 may act as upstream components for AMPK activation and HIF-1α induction under the influence of H_2O_2. The signaling pathway involving HIF-1α, AMPK, JNK and JAK2 was further confirmed by a molecular approach (Figure 6D). Expression of a dominant negative form of either JNK or JAK2 distinctively blocked H_2O_2-induced HIF-1α induction, as well as AMPK activation. The potency of each dominant negative form was confirmed by examining the phosphorylation level of its cellular substrates, c-Jun for JNK and STAT3 for JAK2. Consistent with the results obtained by a pharmacological approach (Figure 6B and C), AMPK inhibition by expression of its dominant negative form did not affect either JNK or JAK2 kinase activity (Figure 6D). Moreover, our results suggest that JNK acts as an upstream of JAK2 under the condition: JNK inhibition led to JAK2 inhibition, but JAK inhibition did not affect JNK activity (Figure 6D). As the result, our data indicate that AMPK, JNK and JAK2 are implicated in the event of the H_2O_2-induced HIF-1α expression, in which JNK and JAK2 act as upstream component in the signaling pathway leading to AMPK activation.

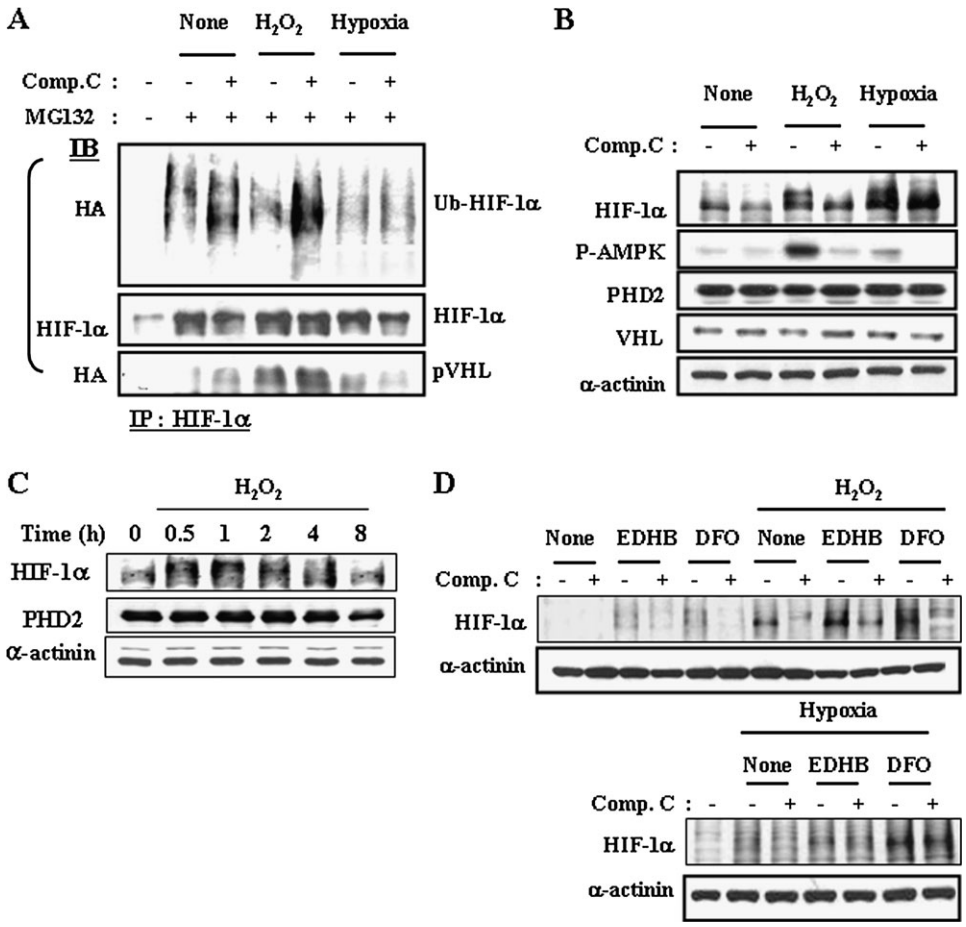

Fig. 5. Effect of AMPK inhibition on HIF-1α ubiquitination and its interaction with pVHL. (**A**) DU145 cells were transiently transfected with plasmid of HA-Ubiquitin or HA-pVHL. After 24 h, the cells were exposed to 0.5 mM H_2O_2 or 1% hypoxia for 1 h, followed by 30 min incubation of 10 μM MG132. Total cell extracts were immunoprecipitated using anti-HIF-1α antibody. The immunocomplex was then analyzed by immunoblotting with anti-HA antibody or anti-HIF-1α antibody. IP, immunoprecipitation; IB, immunoblot; Ub-HIF-1α, ubiquitinated HIF-1α. (**B**) DU145 cells were exposed to 0.5 mM H_2O_2 or 1% hypoxia for 1 h in the absence or presence of compound C (20 μM, Comp.C), and then total cell extracts were subjected to immunoblot assay using antibodies specific to HIF-1α, P-AMPK, P-ACC, PHD2, pVHL and α-actinin. (**C**) DU145 cells were exposed to 0.5 mM H_2O_2 for the indicated times, and then total cell extracts were subjected to immunoblot assay using antibodies specific to HIF-1α, PHD2 and α-actinin. (**D**) DU145 cells were pretreated with 500 μM ethyl 3,4-dihyrdoxybenzoate or 100 μM DFO for 30 min and followed by 0.5 mM H_2O_2 (upper panel) or 1% hypoxia (lower panel) for 1 h. Whole-cell lysates were subjected immunoblot analysis using anti-HIF-1α and anti-α-actinin antibody.

Discussion

Accumulating evidence suggests that the cumulative production of ROS is common for many types of cancer and that ROS play a critical role in cancer development (38,39). Moreover, the high level of ROS in cancer cells was also associated with increased angiogenesis, invasion and metastasis. As HIF-1 plays a central role in cancer development and is primarily regulated by oxygen tension, the link between ROS and HIF-1 regulation has been widely investigated (10). However, the role of ROS is quite controversial, and the mechanism underlying the HIF-1 regulation by ROS is not completely understood yet.

In the present study, we presented a novel and distinct regulatory mechanism for HIF-1α stabilization in response to ROS, in which AMPK plays important roles. To date, the role of ROS in HIF function seems to be complex according to their sources. Some hormones and growth factors, such as insulin and angiotensin II, are reported to produce cellular ROS, which are indispensable to increases of HIF-1α protein translation in normoxia (40,41). However, our results showed that accumulation of HIF-1α in response to exogenic ROS-generating molecules, such as H_2O_2 and menadione, relied on protein turnover rate (Figure 3), which is consistent with the previous notion of ROS in the stabilization of the protein (13–15). Hypoxia and ROS accumulated HIF-1α protein in post-translational level, especially by protein stabilization, which was confirmed by the treatment of protein synthesis inhibitor (Figure 3B and C) or metabolic labeling (Figure 3A) in DU145 cells, whereas insulin induced HIF-1α protein in a translation level as previously reported. These results indicate that HIF-1α is regulated by highly complex and diverse regulation mechanisms in responses to the stimuli. Moreover, although hypoxia and ROS induced HIF-1α stabilization to accumulate, the role of AMPK was shown to be different to each response (Figure 2). We found that AMPK was required for ROS-induced HIF-1α induction (Figure 2), stabilization (Figure 3) and transcriptional activation (Figure 4), whereas AMPK activity was involved only in HIF-1 transcriptional activation under hypoxia condition (Figure 4). These differential effects of AMPK on HIF-1α accumulation in response to ROS and hypoxia, respectively, were also observed in various cancer cell lines (Figure 2C), where only ROS-induced HIF-1α accumulation is sensitive to AMPK activity, whereas hypoxic-induced one is not affected by AMPK inhibition. Therefore, AMPK-dependent HIF-1α accumulation in response to ROS appears to be quite a widespread phenomena rather than certain cell type specific.

It has been extensively explained that oxygen tension is a dominant switch to control PHD activity, but accumulating reports also showed

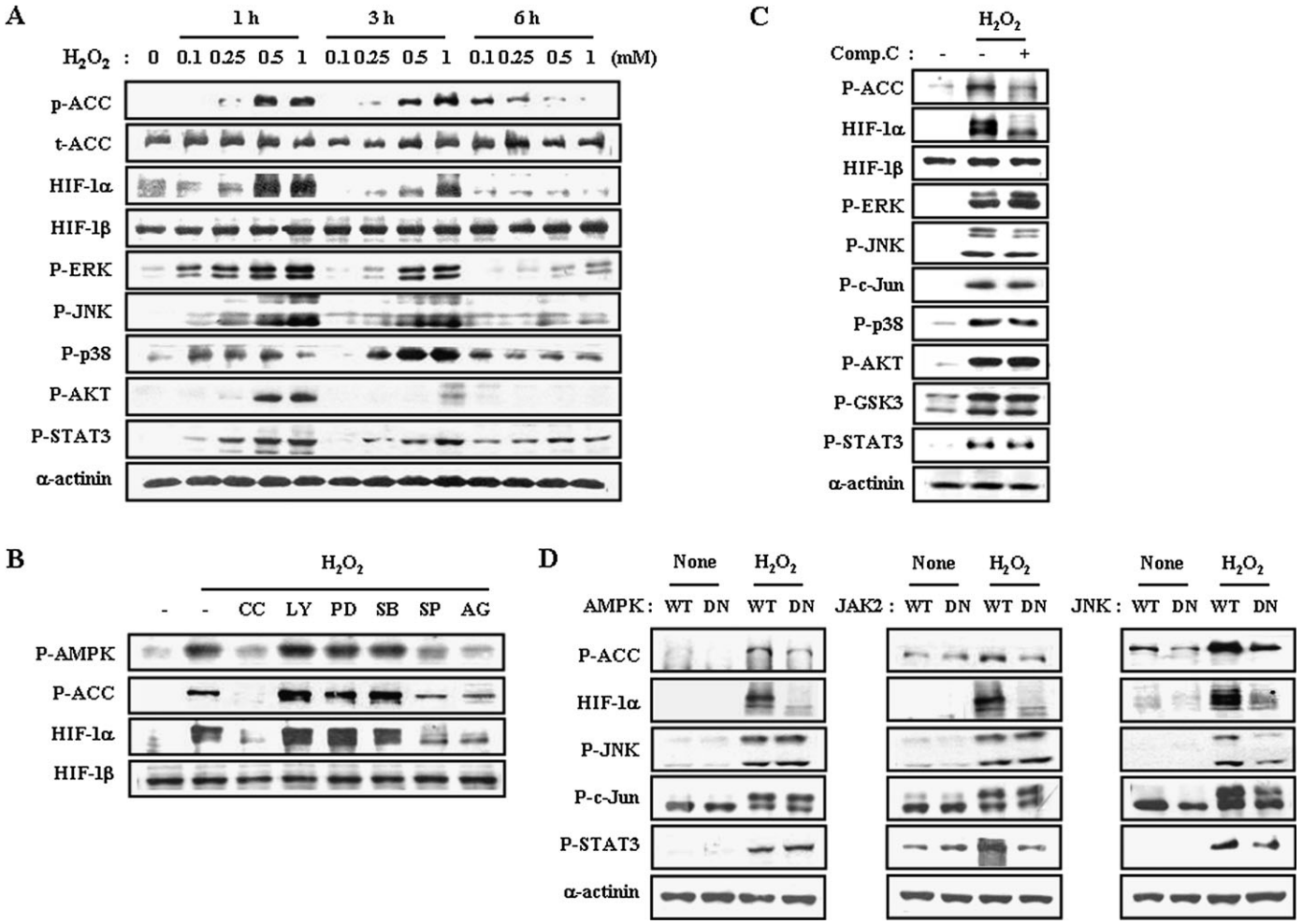

Fig. 6. JNK and JAK2 pathway acts as upstream of AMPK in ROS-induced HIF-1α expression. (**A**) DU145 cells treated with varying concentrations and times of H_2O_2. (**B** and **C**) DU145 cells exposed to H_2O_2 (0.5 mM) for 1 h in the presence of compound C (CC; 20 μM), PD98059 (PD; 25 μM), SP600125 (SP; 25 μM), SB202190 (SB; 25 μM), LY294002 (LY; 25 μM) or AG490 (AG; 50 μM). (**D**) DU145 cells were transiently transfected with wild-type (WT) or dominant negative (DN) plasmid of AMPK and JAK2 and were also stably transfected with JNK1-WT or JNK1-DN plasmid. After 24 h post-transfection, cells were exposed to 0.5 mM H_2O_2 for 1 h. Under these conditions, total cell extracts were subjected to immunoblot assay using anti-phosphospecific AMPK (P-AMPK) ACC (P-ACC), ERK (P-ERK), JNK (P-JNK), p38 (P-p38), AKT (P-AKT), STAT3 (P-STAT3), GSK-3 (P-GSK3) and c-Jun (P-c-Jun) antibodies. The protein level of HIF-1α, HIF-1β, total ACC (t-ACC) and α-actinin were also determined by immunoblot assay.

that ROS and some metabolites, such as succinate and fumarate, inhibited PHD activity through modulation of its cofactors iron and 2-oxo-glutarate availability (42,43). In this study, inhibition of AMPK activity resulted in the increase of HIF-1α ubiquitination and HIF-1 α–pVHL interaction under H_2O_2, which was not observed in cells challenged with hypoxia (Figure 5A). Thus, to understand molecular mechanism underlying HIF-1α stabilization in response to ROS, first, we hypothesized that PHD might be an attractive target to mediate the effect of AMPK on HIF-1α stabilization. However, we found that in the presence of PHD inhibitors, compound C still blocked HIF-1α protein stabilization induced by H_2O_2 but not by hypoxia (Figure 5D), indicating that HIF-1α protein accumulation by PHD inhibitors can be overcome by inhibition of AMPK in ROS condition. This suggests that AMPK-dependent pathway appears to be stronger than inhibition of PHD for the ROS-induced HIF-1α protein stabilization and it is our speculation that other molecules might be involved in AMPK action on HIF-1α protein. Second, several protein kinases including ERK and p38 were reported to directly phosphorylate HIF-1α protein (32–34). However, these kinases were not involved in HIF-1α stabilization and AMPK activation induced by H_2O_2 in DU145 cells (Figure 6B and C). Third, recently, phosphorylation of pVHL by GSK-3β is reported to be associated with its function, where authors showed that phosphorylated pVHL was defective in binding to HIF-2α and its targeting for degradation (44). However, our data showed that GSK-3β did not act downstream of AMPK under H_2O_2 condition (Figure 6C), implying that GSK-3β-mediated phosphorylation of pVHL is not probably involved in AMPK action. Some of the possible scenarios are that the activated AMPK may directly phosphorylate VHL and/or HIF-1α to increase HIF-1α stabilization by preventing HIF-1α–pVHL interaction and HIF-1α ubiquitination in response to ROS. In fact, we are currently investigating these possibilities to further reveal a detailed mechanism of how AMPK activity transmits the positive signal for HIF-1 regulation.

Finally, we verified upstream molecules to regulate AMPK-dependent HIF-1α induction and function in response to H_2O_2. We showed that inhibition of JNK and JAK2 by pharmacological (Figure 6B) and molecular approaches (Figure 6D) distinctively diminished AMPK activation by H_2O_2, resulting in decrease of HIF-1α protein level. Thus, our results strongly suggest that JNK and JAK2 pathway regulate the ROS-induced HIF-1α expression as an upstream of AMPK signaling.

In conclusion, our findings demonstrate that AMPK is a key determinant of HIF-1 functions in response to ROS and hypoxia. Further study on the mechanisms underlying the differential role of AMPK in HIF-1 regulation will provide AMPK as a valuable molecular target for the anticancer therapy.

Funding

The National R and D Program for Cancer Control, Ministry of Health and Welfare (0620080-1); Korea Science and Engineering Foundation grants funded by the Korea government [R13-2002-020-02003-0(2007), 01-2006-000-10517-0].

Acknowledgements

Conflict of Interest Statement: None declared.

References

1. Pouyssegur,J. *et al*. (2006) Hypoxia signalling in cancer and approaches to enforce tumour regression. *Nature*, **441**, 437–443.
2. Wang,G.L. *et al*. (1995) Hypoxia-inducible factor 1 is a basic-helix-loop-helix-PAS heterodimer regulated by cellular O2 tension. *Proc. Natl Acad. Sci. USA.*, **92**, 5510–5514.
3. Bruick,R.K. *et al*. (2001) A conserved family of prolyl-4-hydroxylases that modify HIF. *Science*, **294**, 1337–1340.
4. Berra,E. *et al*. (2006) The hypoxia-inducible-factor hydroxylases bring fresh air into hypoxia signalling. *EMBO Rep.*, **7**, 41–45.
5. Acker,T. *et al*. (2006) The good, the bad and the ugly in oxygen-sensing: ROS, cytochromes and prolyl-hydroxylases. *Cardiovasc. Res.*, **71**, 195–207.
6. Ivan,M. *et al*. (2001) HIFalpha targeted for VHL-mediated destruction by proline hydroxylation: implications for O2 sensing. *Science*, **292**, 464–468.
7. Dery,M.A. *et al*. (2005) Hypoxia-inducible factor 1: regulation by hypoxic and non-hypoxic activators. *Int. J. Biochem. Cell Biol.*, **37**, 535–540.
8. Richard,D.E. *et al*. (2000) Nonhypoxic pathway mediates the induction of hypoxia-inducible factor 1alpha in vascular smooth muscle cells. *J. Biol. Chem.*, **275**, 26765–26771.
9. Gorlach,A. *et al*. (2001) Thrombin activates the hypoxia-inducible factor-1 signaling pathway in vascular smooth muscle cells: role of the p22(phox)-containing NADPH oxidase. *Circ. Res.*, **89**, 47–54.
10. Kietzmann,T. *et al*. (2005) Reactive oxygen species in the control of hypoxia-inducible factor-mediated gene expression. *Semin. Cell Dev. Biol.*, **16**, 474–486.
11. Hool,L.C. *et al*. (2002) Decreasing cellular hydrogen peroxide with catalase mimics the effects of hypoxia on the sensitivity of the L-type Ca2+ channel to beta-adrenergic receptor stimulation in cardiac myocytes. *Circ. Res.*, **91**, 601–609.
12. Vaux,E.C. *et al*. (2001) Regulation of hypoxia-inducible factor is preserved in the absence of a functioning mitochondrial respiratory chain. *Blood*, **98**, 296–302.
13. Kietzmann,T. *et al*. (1996) Regulation of the gluconeogenic phosphoenolpyruvate carboxykinase and glycolytic aldolase A gene expression by O2 in rat hepatocyte cultures. Involvement of hydrogen peroxide as mediator in the response to O2. *FEBS Lett.*, **388**, 228–232.
14. Guzy,R.D. *et al*. (2005) Mitochondrial complex III is required for hypoxia-induced ROS production and cellular oxygen sensing. *Cell Metab.*, **1**, 401–408.
15. Chandel,N.S. *et al*. (2000) Reactive oxygen species generated at mitochondrial complex III stabilize hypoxia-inducible factor-1alpha during hypoxia: a mechanism of O2 sensing. *J. Biol. Chem.*, **275**, 25130–25138.
16. Huang,L.E. *et al*. (1996) Activation of hypoxia-inducible transcription factor depends primarily upon redox-sensitive stabilization of its alpha subunit. *J. Biol. Chem.*, **271**, 32253–32259.
17. Chang,T.C. *et al*. (2005) Stabilization of hypoxia-inducible factor-1{alpha} by prostacyclin under prolonged hypoxia via reducing reactive oxygen species level in endothelial cells. *J. Biol. Chem.*, **280**, 36567–36574.
18. Srinivas,V. *et al*. (2001) Oxygen sensing and HIF-1 activation does not require an active mitochondrial respiratory chain electron-transfer pathway. *J. Biol. Chem.*, **276**, 21995–21998.
19. Kemp,B.E. *et al*. (2003) AMP-activated protein kinase, super metabolic regulator. *Biochem. Soc. Trans.*, **31**, 162–168.
20. Marsin,A.S. *et al*. (2002) The stimulation of glycolysis by hypoxia in activated monocytes is mediated by AMP-activated protein kinase and inducible 6-phosphofructo-2-kinase. *J. Biol. Chem.*, **277**, 30778–30783.
21. Choi,S.L. *et al*. (2001) The regulation of AMP-activated protein kinase by H(2)O(2). *Biochem. Biophys. Res. Commun.*, **287**, 92–97.
22. Lee,M. *et al*. (2003) AMP-activated protein kinase activity is critical for hypoxia-inducible factor-1 transcriptional activity and its target gene expression under hypoxic conditions in DU145 cells. *J. Biol. Chem.*, **278**, 39653–39661.
23. Yun,H. *et al*. (2005) Glucose deprivation increases mRNA stability of vascular endothelial growth factor through activation of AMP-activated protein kinase in DU145 prostate carcinoma. *J. Biol. Chem.*, **280**, 9963–9972.
24. Lee,M. *et al*. (2006) Critical roles of AMP-activated protein kinase in the carcinogenic metal-induced expression of VEGF and HIF-1 proteins in DU145 prostate carcinoma. *Biochem. Pharmacol.*, **72**, 91–103.
25. Watanabe,N. *et al*. (2003) Autoxidation of extracellular hydroquinones is a causative event for the cytotoxicity of menadione and DMNQ in A549-S cells. *Arch. Biochem. Biophys.*, **411**, 145–157.
26. Zhou,G. *et al*. (2001) Role of AMP-activated protein kinase in mechanism of metformin action. *J. Clin. Invest.*, **108**, 1167–1174.
27. Treins,C. *et al*. (2002) Insulin stimulates hypoxia-inducible factor 1 through a phosphatidylinositol 3-kinase/target of rapamycin-dependent signaling pathway. *J. Biol. Chem.*, **277**, 27975–27981.
28. Gao,N. *et al*. (2002) p38 Signaling-mediated hypoxia-inducible factor 1alpha and vascular endothelial growth factor induction by Cr(VI) in DU145 human prostate carcinoma cells. *J. Biol. Chem.*, **277**, 45041–45048.
29. Hur,E. *et al*. (2001) Mitogen-activated protein kinase kinase inhibitor PD98059 blocks the trans-activation but not the stabilization or DNA binding ability of hypoxia-inducible factor-1alpha. *Mol. Pharmacol.*, **59**, 1216–1224.
30. McMahon,S. *et al*. (2006) Transforming growth factor beta1 induces hypoxia-inducible factor-1 stabilization through selective inhibition of PHD2 expression. *J. Biol. Chem.*, **281**, 24171–24181.
31. Gerald,D. *et al*. (2004) JunD reduces tumor angiogenesis by protecting cells from oxidative stress. *Cell*, **118**, 781–794.
32. Richard,D.E. *et al*. (1999) p42/p44 mitogen-activated protein kinases phosphorylate hypoxia-inducible factor 1alpha (HIF-1alpha) and enhance the transcriptional activity of HIF-1. *J. Biol. Chem.*, **274**, 32631–32637.
33. Mylonis,I. *et al*. (2006) Identification of MAPK phosphorylation sites and their role in the localization and activity of hypoxia-inducible factor-1alpha. *J. Biol. Chem.*, **281**, 33095–33106.
34. Kwon,S.J. *et al*. (2005) Signal pathway of hypoxia-inducible factor-1alpha phosphorylation and its interaction with von Hippel-Lindau tumor suppressor protein during ischemia in MiaPaCa-2 pancreatic cancer cells. *Clin. Cancer Res.*, **11**, 7607–7613.
35. Comerford,K.M. *et al*. (2004) c-Jun NH2-terminal kinase activation contributes to hypoxia-inducible factor 1alpha-dependent P-glycoprotein expression in hypoxia. *Cancer Res.*, **64**, 9057–9061.
36. Mazure,N.M. *et al*. (1997) Induction of vascular endothelial growth factor by hypoxia is modulated by a phosphatidylinositol 3-kinase/Akt signaling pathway in Ha-ras-transformed cells through a hypoxia inducible factor-1 transcriptional element. *Blood*, **90**, 3322–3331.
37. Jung,J.E. *et al*. (2005) STAT3 is a potential modulator of HIF-1-mediated VEGF expression in human renal carcinoma cells. *FASEB J.*, **19**, 1296–1298.
38. Storz,P. (2005) Reactive oxygen species in tumor progression. *Front. Biosci.*, **10**, 1881–1896.
39. Behrend,L. *et al*. (2003) Reactive oxygen species in oncogenic transformation. *Biochem. Soc. Trans.*, **31**, 1441–1444.
40. Zhou,Q. *et al*. (2007) Reactive oxygen species regulate insulin-induced VEGF and HIF-1alpha expression through the activation of p70S6K1 in human prostate cancer cells. *Carcinogenesis*, **28**, 28–37.
41. Page,E.L. *et al*. (2002) Induction of hypoxia-inducible factor-1alpha by transcriptional and translational mechanisms. *J. Biol. Chem.*, **277**, 48403–48409.
42. Pan,Y. *et al*. (2007) Multiple factors affecting cellular redox status and energy metabolism modulate hypoxia-inducible factor prolyl hydroxylase activity *in vivo* and *in vitro*. *Mol. Cell. Biol.*, **27**, 912–925.
43. King,A. *et al*. (2006) Succinate dehydrogenase and fumarate hydratase: linking mitochondrial dysfunction and cancer. *Oncogene*, **25**, 4675–4682.
44. Hergovich,A. *et al*. (2006) Priming-dependent phosphorylation and regulation of the tumor suppressor pVHL by glycogen synthase kinase 3. *Mol. Cell. Biol.*, **26**, 5784–5796.

Received September 10, 2007; revised January 24, 2008; accepted January 26, 2008